VOL. 11, NO. 16, AUGUST 2016 ISSN 1819-6608
ARPN Journal of Engineering and Applied Sciences

www.arpnjournals.com

SHARK SKIN FOR ENHANCING THE FLOW OF UNDERWATER VEHICLES

Hayder A. Abdulbari[1,2], Hassan D. Mahammed[1], Zulkefli B. Yaacob[1] and Wafaa K. Mahmood[2]
[1]Faculty of Chemical and Natural Resources Engineering, Universiti Malaysia Pahang, Gambang, Kuantan, Pahang, Malaysia
[2]Center of Excellence for Advanced Research in Fluid Flow, Universiti Malaysia Pahang, Gambang, Kuantan, Pahang, Malaysia
E-Mail: hayder.bari@gmail.com

ABSTRACT

Nature is full of flow control examples and has long provided subjects of interest in the field of fluid mechanics. From birds flying in a V-formation, to feathers on a bird, to scales on a butterfly wing, to the skin of marine creatures, such as octopus, fish, dolphins, and sharks that provide abundant shape resources for restructuring the surfaces to enhance flow of underwater vehicles. Riblets like shark skin have gained renewed interest in academic fields of study and in industry due to several advantages in manipulating the turbulence boundary layer. Drag measurements have been carried out in a water channel over flat plate. In these experiments, smooth plate was compared to riblet-structured films. This was done for different dimension of V-groove riblets fixed on the surface with the riblet direction aligned with the flow. The lateral spacing between the triangular shaped riblets varied between 800µm and 2000µm. The drag reduction experiments show that the maximum drag reduction rate of up to 11% over the velocities tested.

Keywords: drag reduction, skin friction, riblets, geometry.

INTRODUCTION

The For the decades, the rising energy costs due to the oil crisis and limited energy resources have led researchers to seek and develop new techniques to reduce vehicle drag. Since then, viscous drag reduction has been a very active field of study (Gad-el-Hak, 1989). In underwater vehicle applications, energy is used to move a solid body through a fluid. A substantial amount of energy is expended to overcome the drag force (Gad-el-Hak, 2007; Zakin & Ge, 2010). This drag is typically referred to as skin friction and represents a significant component of the total drag force. It comprises nearly 50% of the total drag force on commercial aircraft, 90% of the total drag force on submarines, and 100% of the total drag force in long distance pipelines (Cousteix, 1992; Gallego & Shah, 2009; Lee & Lee, 2001).

Swimming style and body form of sharks has been subject of interest since decades. Over millions of years of evolution, such forms and swimming techniques have been the inspiration of many inventions in our life today. The inspiration comes from the observation of the swimming technique of sharks, Reif (1978); (1982) was the first who comes up with the concept of using groove like shirk skin to reduce the drag force.

The agility of a shark enables it to maneuver and change direction instantly, regardless of its speed. It has got a sleek and torpedo-like body profile that helps in minimizing drag. Additionally, it has been suggested that the scales covering the shark could be a source of further drag reduction and flow separation control. A shark scale contains special sized and spaced grooves that run parallel to the flow direction and act as riblets over its surface, thereby decreasing drag by deterring cross flow (Bechert *et al.,* 2000; B. Dean & Bhushan, 2010; D. Zhang *et al.,* 2011).

Riblet like shark skin surfaces have been studied for more than 30 years, both experimentally and computationally (Ball, 1999; Bechert, 1987; Bechert & Bartenwerfer, 1989; Bechert *et al*., 2000; Bechert *et al.,* 1997; Bechert *et al*., 1992; Bharat Bhushan, 2012; Bixler & Bhushan, 2013; Büttner & Schulz, 2011; Chen *et al.,* 2014; B. Dean & Bhushan, 2010; Brian Dean & Bhushan, 2012; Lynn *et al.,* 1991; Reif, 1978, 1982; Reif & Dinkelacker, 1982; Videler, 1995; D.-y. Zhang *et al*., 2011; D. Zhang *et al.,* 2011; Zhao *et al.,* 2012).

Available information regarding contribution of geometry to the riblets' ability to reduce skin friction during a fluid flow, provide approval to the use of triangular profile groove (Nitschke, 1983). For instance, investigation on the ability of rectangular profile groove to reduce drag force in a fluid flow did not have any effect on the turbulence (Savill, 1990). On the other hand, the use of a triangular profile grove presented smaller increase in drag force (Sawyer & Winter, 1987). Redesigning of the triangle, by reducing spacing of the riblets produced a V-groove configuration. A test on the V-groove with a height of 15-20 resulted into a drag reduction of 7% (Beauchamp & Philips, 1988). The positive results obtained after conducting tests on V-groove paved way for farther studies, as researchers began to investigate effectiveness of V-groove in reducing skin friction of the fluid flow (Djenidi *et al.,* 1989). The growing interest resulted in refinement of the test parameters into three rib geometries (Neumann & Dinkelacker, 1991).

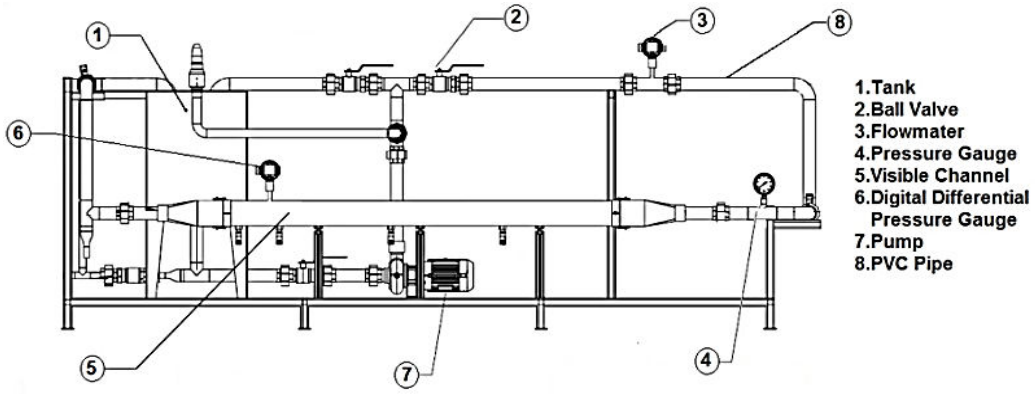

Figure-1. Schematic diagram of the experimental rig.

The three geometries were peak curvature, valley curvature and notched-peak V-groove. After the tests, maximum drag reduction of 8% was attained while using v-groove configuration with valley curvature and sharp peak of h+89 to 20, while spacing being set between 15 and 20 (Vukoslavcevic *et al.,* 1992). Changing the spacing between V-groove down to 13 to 15 resulted in reduction of drag force of between 7-8% (Dong & Ding, 1990).

A number of studies have investigated various shapes and groove dimension and have shown that these surface geometry can reduce the viscous drag (Abdulbari *et al.,* 2015; B. Bhushan, 2009; Bushnell, 2003; B. Dean & Bhushan, 2010).

It is of interest to understand how these surface modifications manipulate the boundary layer near wall by energy transfer which is affected by the natural interaction dynamics of the fluid along the solid boundary. The purpose of this study was to investigate the drag reducing effect of riblet surface on marine vehicles.

MATERIALS AND METHODS

Riblets fabrication

In Four models were studied and the dimensions of these riblets are given in Table 1. The plates used in the test were aluminium with dimensions (0.16 × 0.08)m fabricated by Wire-cut EDM. A single geometry of triangular groove riblets was tested. The grooves of four plates have same height (h) equal to 800µm and the spacing (s) equal to (800, 1000, 1333, 2000) µm. The total film thickness measured to the peaks -of the grooves is 0.008m

Table-1. Dimension of fabricated grooves.

Triangular groove	Model	h (µm)	s (µm)
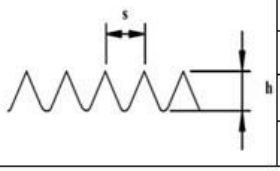	Model A	800	800
	Model B	800	1000
	Model C	800	1333
	Model D	800	2000

Experimental apparatus

A closed loop system as shown in the schematic diagrams, Figure 1, was designed to hold water and consists of a tank that has a 70 liters capacity connected to a centrifugal pump. Water is then pumped from the centrifugal pump, from the supply tank, into the PVC pipes with 2 inches size, then through the transparent channel and into the supply tank again. The main components of this experimental rig include: supply tank, flow meter, centrifugal pumps, PVC pipes, control panel, ball valves, pressure transmitter and a pressure gauge.

The supply tank is rectangular in shape and has the size 500 mm long by 300mm wide and a depth of 520mm with a capacity of 17 liters. The line of suction for the centrifugal pump is then provided at the bottom of the supply tank. The centrifugal pump is a self-priming type and it has the capability to drive the primary fluid at a rate of 36 m^3/hr.

The rectangular channel of the experimental rig has been designed and fabricated in such a manner that there are four transparent polycarbonate plates with dimensions (2 × 0.12× 0.01)m, which have been used to fabricate the channel as shown in Figure 2.

Acrylic was selected for fabrication of all sections of the channel, due to strength and transparency in addition to acrylic welding are soften the plate surfaces so they merge, and the molecules between the two pieces become one which gave much more strength to the channel and prevent leakages. Four pressure tabs are placed at the bottom surface of the channel used for the measurement of pressure drop. These tabs made the test sections where $0.16m$ placed after two sections of $0.55m$ in order to get full turbulence flow. The system also has six ball valves that are strategically located at the points of entry and exit of the water and are primarily to regulate the flow of water. Pressure transmitters are connected to the first test section with $0.16m$ length and the pressure drop has been taken for section over smooth plate and rib surfaces.

The experimental rig also has a flow meter that is located in the flow duct.

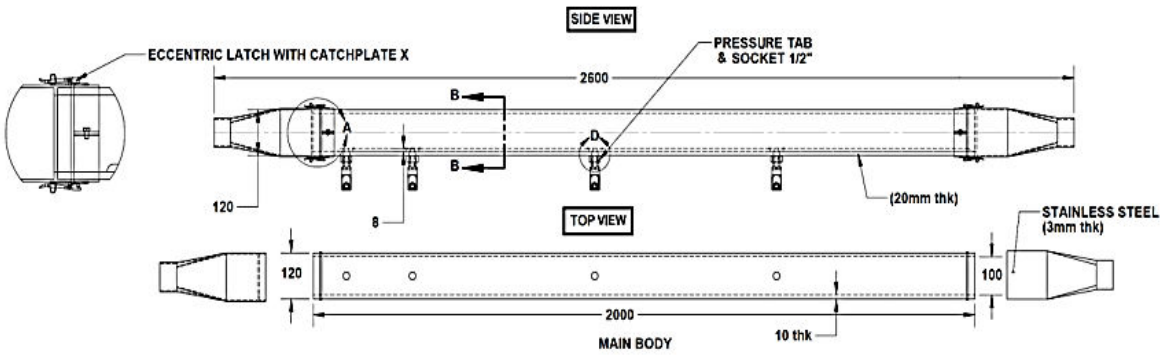

Figure-2. Schematic of testing section.

It basically records the amount of water flowing through the rig before it proceeds on to the pressure transmitter. The control panel located away from the flow duct allows the control and recording of any data that is transmitted from the rig including the rate of flow and the pressure drop in the system.

The primary path of the rig starts from the water supply tank through the 2'' ball valves that allow the entry of the water and are situated on the pump. If an attempt is made to increase the flow rate by closing the valve, the water will flow back to the tank and therefore the valve must remain open. The second valve allows water to flow through at a rate of between 4 and 16 cubic meters per hour. The pipes used in the rig are primary of the PVC type.

Measurement

The skin friction coefficients (C*f*) and Reynolds numbers (Re) calculated from wall shear stress and flow rate measurements by using following equations,

$$Cf = \frac{2\tau_w}{\rho\, u^2} \text{ and } Re = \frac{u\, D_h}{\upsilon} \quad (1)$$

Where (u) is mean velocity $(m/\sec)$, (υ) is the kinematic viscosity of water $(m^2/\sec)$, (ρ) is the density of water (Kg/m^3) and (τ_w) is the wall shear stress in a fully developed pipe flow was defined by (Perry *et al*. 1963). This equation relates the wall shear stress to the pressure drop during the turbulent flow inside pipelines.

$$\tau_w = \frac{\Delta p\, D_h}{4L} \quad (2)$$

The height and spacing of the grooves in wall units are calculated by using Walsh (1982) identification in terms of wall units as non-dimensional height (h^+) and spacing (s^+), as;

$$h^+ = \frac{h\, u}{\nu}\sqrt{\frac{C_f}{2}} \text{ and } s^+ = \frac{s\, u}{\nu}\sqrt{\frac{C_f}{2}}, \quad (3)$$

where (C_f) is local skin friction coefficient, (s) is peak to peak spacing of riblets and (h) is the valley to peak height of riblets.

The percentage drag reduction (DR %) is defined as:

$$\text{DR\%} = \left(\frac{\Delta P_{Smooth} - \Delta P_{riblet}}{\Delta P_{Smooth}}\right) \times 100 \quad (4)$$

The diameter used in the calculations Reynolds number and friction coefficient is defined as Hydraulic diameter $D_h = 4\frac{A}{p}$ Where (A) is area section of the duct and (p) is wetted perimeter of the duct.

RESULTS AND DISCUSSION

Experimental work has been undertaken to estimate the contribution of pressure drop components on smooth and rib surfaces. The impacts of riblets dimension, height and space were studied and their influences on each component of pressure drop and on total drag reduction.

In Figure 3 a comparison of the pressure drop measured across the smooth plate and all riblet surfaces tested in channel is shown and plotted against the Reynolds number which has been calculated by using equation (1).

Several features are apparent from the results presented, Model (A) shows no beneficial trend is demonstrated comparing to smooth surface for Reynolds number range between $(1 \times 10^4 - 3 \times 10^4)$ moreover, it was noted increasing in pressure drop when Reynolds number more than (3×10^4).

On the other hand, the results of models (B, C, and D) shows decreasing in pressure drop comparing to smooth surface especially when Reynolds number more than (3×10^4). Model (C) shows best decreasing in pressure drop compare to smooth and rib plates.

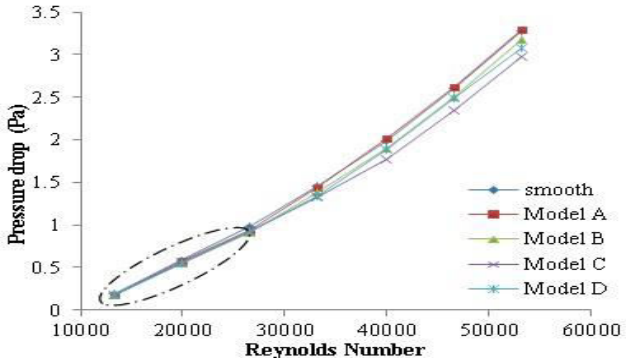

Figure-3. Pressure drop comparison over smooth and triangular groove.

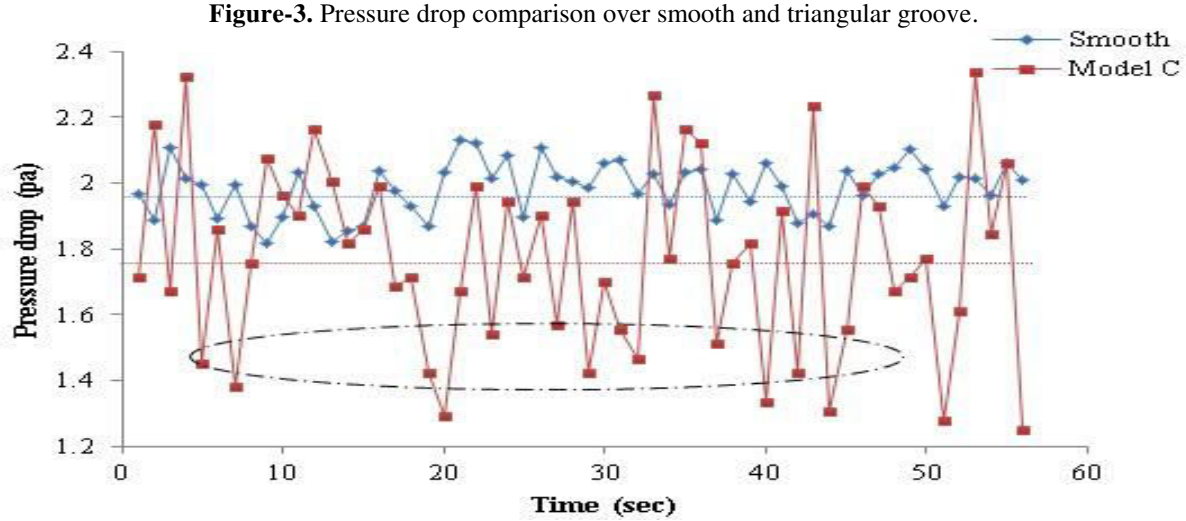

Figure-4. Effect of time on pressure drop over smooth and triangular groove modal (C) at Reynolds number = 4×10^4.

Figure-4 shows the pressure drop fluctuation over smooth plate and triangular riblet plate model (C). In turbulent flow, because of the fluctuations, every velocity and pressure term in momentum and energy equations is a rapidly varying random function of time and space. The frequency and pressure drop become lower in same period of time at same Reynolds number. The variance shows the frequency been reduced from 1.98 to 1.77. Lowering the pressure drop is an essential reason of doing this research.
The drag reduction observed for all model and the maximum drag reduction recorded was 10.62% for model (C), which occurred for $h^+ = 15.97$ and $s^+ = 26.61$..

The present measurements of riblet drag reduction shows that the percentage drag reduction increases by increasing the h^+ for most of the tested riblets until a certain value where the percentage drag reduction start to descend.

After that and by a further increase in the value of the h^+ start to decline in most cases due to the strong action of these turbulent structures over riblets, where riblets no longer could modify these structures, which is dependent on the properties of the particular boundary layer .
reaching a maximum point or maximum performance " which might be considered as optimum performance for this point only".

Where in a certain range of h^+ , the percentage drag reduction start to increase with any increase in the h^+ which means increasing the turbulence spectrum and
It proves that riblets with triangular shape, have dimensions h=800 μm, s=1333 μm is a good pressure drop reducer hence increased the percentage of drag reduction.

Figure-5 shows the data plotted as a function of h^+ and the percentage of drag reduction results calculated. The riblet size in nondimensional wall units was then estimated from equation (3) and the percentage of drag reduction was estimated from equation (4).

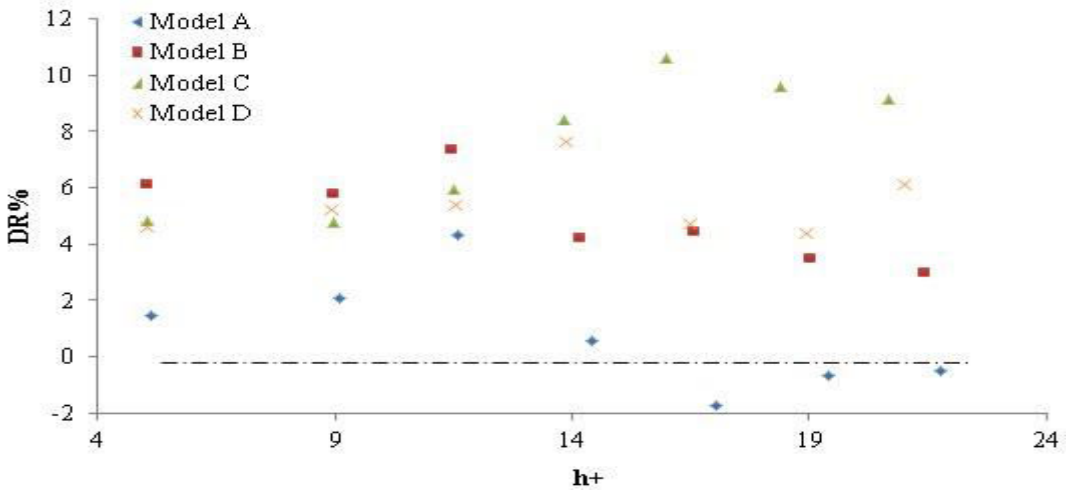

Figure-5. Percentage of drag reduction of triangular groove.

CONCLUSION

As a conclusion for the work, the investigation of using riblets like shark skin to reduce the drag force in water flow where the pressure drop over smooth and rib surfaces is measured. The present measurements of riblet drag reduction shows that the pressure drop decreases by increasing the Reynolds number for models (B, C, D).Model (C) has the high potential in enhancing the flow in under water vehicles as the riblets with triangular shape and with for h^+=15.97 shows pressure drop less than the pressure drop over smooth.

ACKNOWLEDGEMENTS

This work was supported financially by Universiti Malaysia Pahang (UMP) through the Fundamental Research Grant.

REFERENCES

[1] Abdulbari, H. A., Mahammed, H. D., & Hassan, Z. B. Y. (2015). Bio-Inspired Passive Drag Reduction Techniques: A Review. ChemBioEng Reviews, 2(3), 185-203.

[2] Ball, P. (1999). Engineering shark skin and other solutions. Nature, 400(6744), 507-509.

[3] Beauchamp, C., & Philips, R. (1988). Riblet and polymer drag reduction on an axisymmetric body. Paper presented at the Symposium on Hydrodynamic Performance Enhancement for Marine Applications, Newport, Rhode Island.

[4] Bechert, D. W. (1987, September 15–17). Experiments on three-dimensional riblets. Paper presented at the International conference on Turbulent Drag Reduction by Passive Means, London, England.

[5] Bechert, D. W., & Bartenwerfer, M. (1989). The viscous flow on surfaces with longitudinal ribs. Journal of Fluid Mechanics, 206(-1), 105-129.

[6] Bechert, D. W., Bruse, M., & Hage, W. (2000). Experiments with three-dimensional riblets as an idealized model of shark skin. Experiments in Fluids, 28(5), 403-412.

[7] Bechert, D. W., Bruse, M., Hage, W., Van Der Hoeven, J. G. T., & Hoppe, G. (1997). Experiments on drag-reducing surfaces and their optimization with an adjustable geometry. Journal of Fluid Mechanics, 338, 59-87.

[8] Bechert, D. W., Hoppe, G., van der Hoeven, J. G. T., & Makris, R. (1992). The Berlin oil channel for drag reduction research. Experiments in Fluids, 12(4-5), 251-260.

[9] Bhushan, B. (2009). Biomimetics: lessons from nature - an overview. Philos Trans A Math Phys Eng Sci, 367(1893), 1445-1486.

[10] Bhushan, B. (2012). Shark skin Surface for Fluid-Drag Reduction in Turbulent Flow. In B. Bhushan (Ed.), Biomimetics (pp. 227-265): Springer Berlin Heidelberg.

[11] Bixler, G. D., & Bhushan, B. (2013). Fluid Drag Reduction with Shark-Skin Riblet Inspired Microstructured Surfaces. Advanced Functional Materials, 23(36), 4507-4528.

[12] Bushnell, D. M. (2003). Aircraft drag reduction—a review. Proceedings of the Institution of Mechanical Engineers, Part G: Journal of Aerospace Engineering, 217(1), 1-18.

[13] Büttner, C. C., & Schulz, U. (2011). Shark skin inspired riblet structures as aerodynamically optimized high temperature coatings for blades of aeroengines. Smart Materials and Structures, 20(9), 094016.

[14] Chen, H., Zhang, X., Che, D., Zhang, D., Li, X., & Li, Y. (2014). Synthetic Effect of Vivid Shark Skin and Polymer Additive on Drag Reduction Reinforcement. Advances in Mechanical Engineering, 2014, 1-8.

[15] Cousteix, J. (1992). Basic concepts on boundary layers (92-17809). In J. Cousteix (Ed.), Special Course on Skin Friction Drag Reduction (AGARD-R-786) (pp. 1- 39). Belgium: Advisory Group for Aerospace Research and Development (AGARD).

[16] Dean, B., & Bhushan, B. (2010). Shark-skin surfaces for fluid-drag reduction in turbulent flow: a review. Philos Trans A Math Phys Eng Sci, 368(1929), 4775-4806.

[17] Dean, B., & Bhushan, B. (2012). The effect of riblets in rectangular duct flow. Applied Surface Science, 258(8), 3936-3947.

[18] Djenidi, L., Liandrat, J., Anselmet, F., & Fulachier, L. (1989). On the Mechanism Involved in a Turbulent Boundary Layer over Riblets. In H.-H. Fernholz & H. E. Fiedler (Eds.), Advances in Turbulence 2 (pp. 438-442). Berlin Heidelberg: Springer.

[19] Dong, Z., & Ding, Y. (1990). Turbulence characteristics in smooth open-channel flow. Science In China Series A-Mathematics Physics Astronomy, 33(2), 244-256.

[20] Gad-el-Hak, M. (1989). The Art and Science of Flow Control. In M. Gad-el-Hak (Ed.), Frontiers in Experimental Fluid Mechanics (Vol. 46, pp. 211-290): Springer Berlin Heidelberg.

[21] Gad-el-Hak, M. (2007). Flow control: passive, active, and reactive flow management. New York: Cambridge University Press.

[22] Gallego, F., & Shah, S. N. (2009). Friction pressure correlations for turbulent flow of drag reducing polymer solutions in straight and coiled tubing. Journal of Petroleum Science and Engineering, 65(3-4), 147-161.

[23] Lee, S. J., & Lee, S. H. (2001). Flow field analysis of a turbulent boundary layer over a riblet surface. Experiments in Fluids, 30(2), 153-166.

[24] Lynn, T. B., Gerich, D. A., & Bechert, D. W. (1991). Direct Drag Measurements in a LEBU Manipulated Flat-Plate Boundary Layer. In A. Johansson & P. H. Alfredsson (Eds.), Advances in Turbulence 3 (pp. 472-480): Springer Berlin Heidelberg.

[25] Neumann, D., & Dinkelacker, A. (1991). Drag measurements on V-grooved surfaces on a body of revolution in axial flow. Applied Scientific Research, 48(1), 105-114.

[26] Nitschke, P. (1983). Experimental investigation of the turbulent flow in smooth and longitudinal grooved tubes (NASA TM77480). Retrieved from Washington, DC, United States:

[27] Reif, W. E. (1978). Types of morphogenesis of the dermal skeleton in fossil sharks. Paläontologische Zeitschrift, 52(1-2), 110-128.

[28] Reif, W. E. (1982). Morphogenesis and function of the squamation in sharks. Neues Jahrbuchfuer Geologie und Palaeontologie, 164(1982), 172-183.

[29] Reif, W. E., & Dinkelacker, A. (1982). Hydrodynamics of the Squamation in Fast Swimming Sharks. Neues Jahrbuch fuer Geologie und Palaeontologie, 16(1982), 184-187.

[30] Savill, A. M. (1990). Drag Reduction by Passive Devices - a Review of some Recent Developments Structure of Turbulence and Drag Reduction (pp. 429-465): Springer Berlin Heidelberg.

[31] Sawyer, W., & Winter, K. (1987, Sept. 15-17). An investigation of the effect on turbulent skin friction of surfaces with streamwise grooves. Paper presented at the Proceedings International Conference on Turbulent Drag Reduction by passive means, London, England.

[32] Videler, J. J. (1995). Body surface adaptations to boundary-layer dynamics. Symp Soc Exp Biol, 49, 1-20.

[33] Vukoslavcevic, P., Wallace, J. M., & Balint, J. L. (1992). Viscous drag reduction using streamwise-aligned riblets. AIAA Journal, 30(4), 1119-1122.

[34] Walsh, M. J. (1982). Turbulent boundary layer drag reduction using riblets 20th Aerospace Sciences Meeting. USA: American Institute of Aeronautics and Astronautics.

[35] Zakin, J. L., & Ge, W. (2010). Polymer and Surfactant Drag Reduction in Turbulent Flows Polymer Physics (pp. 89-127): John Wiley & Sons, Inc.

[36] Zhang, D.-y., Luo, Y.-h., Li, X., & Chen, H.-w. (2011). Numerical simulation and experimental study of drag-reducing surface of a real shark skin. Journal of Hydrodynamics, Ser. B, 23(2), 204-211.

[37] Zhang, D., Li, Y., Han, X., Li, X., & Chen, H. (2011). High-precision bio-replication of synthetic drag reduction shark skin. Chinese Science Bulletin, 56(9), 938-944.

[38] Zhao, D.-Y., Huang, Z.-P., Wang, M.-J., Wang, T., & Jin, Y. (2012). Vacuum casting replication of micro-riblets on shark skin for drag-reducing applications. Journal of Materials Processing Technology, 212(1), 198-2.